UPWARDS

UNDERSTANDING PLANET MARS

Characterization of dust activity from MY 27 to MY 32 observed by the PFS - MEx

Paulina Wolkenberg[1,2], Marco Giuranna[1], Davide Grassi[1], Alessandro Aronica[1], Shohei Aoki[3,4], Diego Scaccabarozzi[5], Bortolino Saggin[5]

[1]Institute for Space Astrophysics and Planetology (IAPS), National Institute of Astrophysics (INAF), Roma, Italy

[2]Centrum Badań Kosmicznych (CBK), Polska Akademia Nauk (PAN), Warsaw, Poland

[3]Department of Geophysics, Graduate school of Science, Tohoku University, Sendai, Japan

[4]Institut d'Aéronomie Spatiale de Belgique, avenue Circulaire 3, 1180 Brussels, Belgium

[5]Department of Mechanics, Politecnico di Milano, Campus of Lecco, Lecco, Italy

Outline

- PFS retrievals, estimation of dust uncertainty, algorithm
- Comparison with TES, THEMIS and MCS data
- Dust activity in different Martian years
- Effect of dust on atmospheric temperatures
- Conclusions

PFS retrievals, estimation of dust uncertainty, algorithm

- PFS measures radiances in the short- and long-wavelength channels. Atmospheric temperatures, aerosol column integrated optical depths and surface temperatures are retrieved from the LWC radiances.
- Retrievals are perfomed by means of the optimal estimation method with Bayesian approach (Grassi et al., 2005). Recently the algorithm was improved and optimized with respect to retrievals of aerosol opacities during dust storms (Wolkenberg et al., 2018, in press)
- Retrieved dust uncertainties are estimated from the final covariance matrix of all retrieved parameters. After analysis of 5000 measurements in different atmospheric conditions and locations we find that standard deviations of dust opacities are strongly depended on surface temperatures. We find two populations of dust standard deviations with respect to surface temperatures.
- Dust uncertainties peak at 0.02 – 0.06 for Ts > 220 K, and at 0.11 for lower surface temperatures.

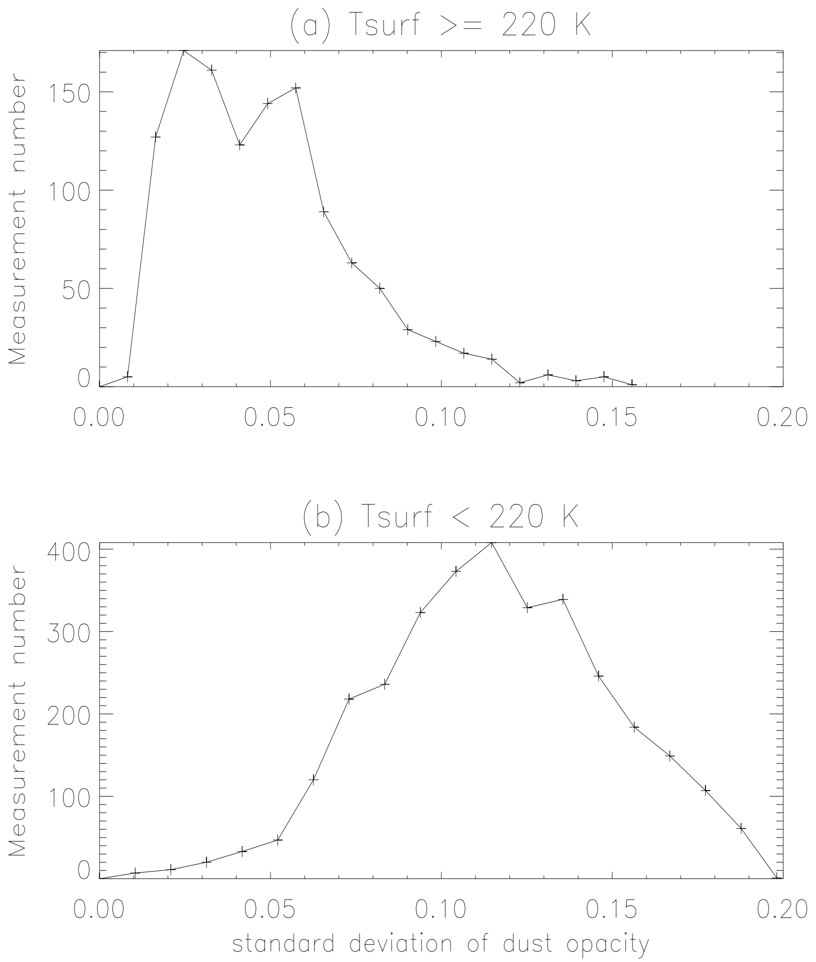

Histograms of standard deviations for dust.

Comparison with TES data

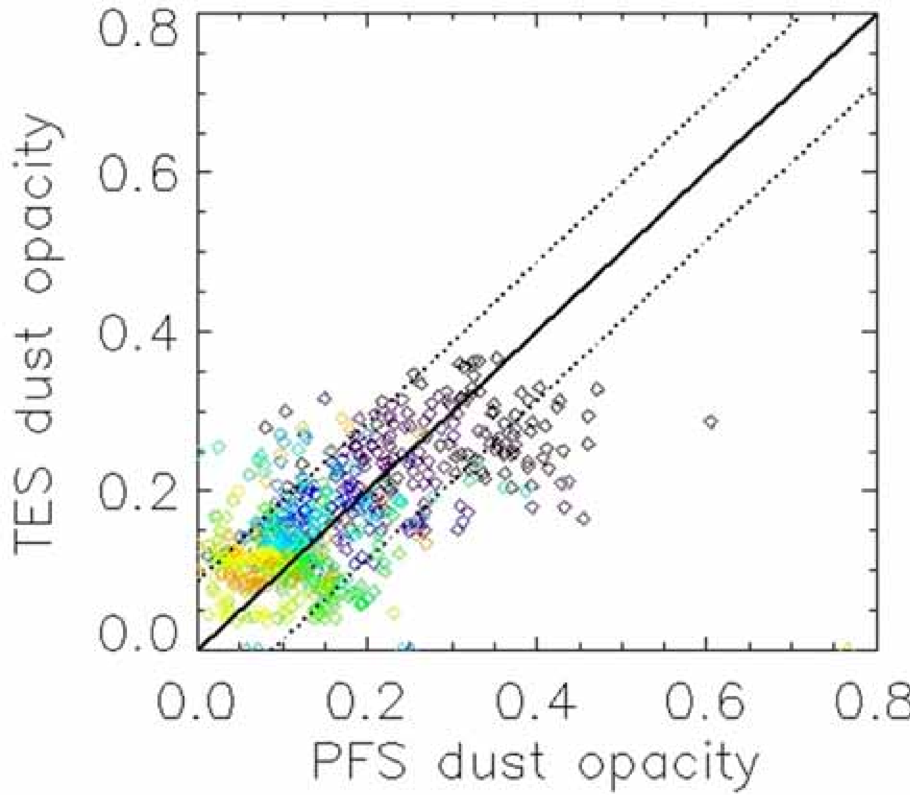

Overlapping interval:
Ls = 330°(MY26) – 80°(MY27

Comparison of zonal mean dust opacities obtained from TES and PFS measurements in MY 26 and MY 27 for intervals: Ls = 330° – 340° (black), Ls = 340° – 350° (dark purple), Ls = 355° – 10° (dark blue), Ls = 10° – 15° (blue), Ls = 15° – 30° (light blue), Ls = 30° – 60° (green), Ls = 60° – 65° (light green), Ls = 65° – 75° (yellow), Ls = 75° – 80° (orange). A combined standard deviation is plotted with a dashed line.

Comparison with TES, THEMIS and MCS data

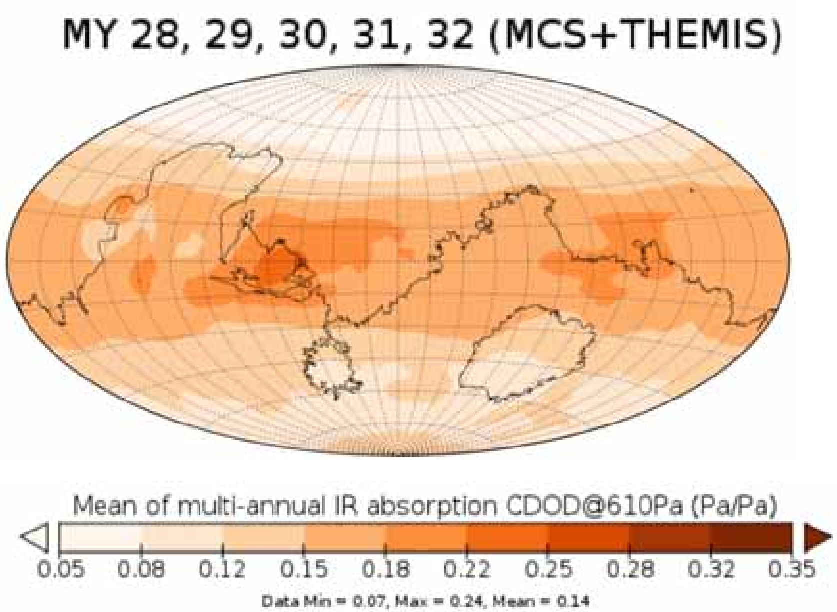

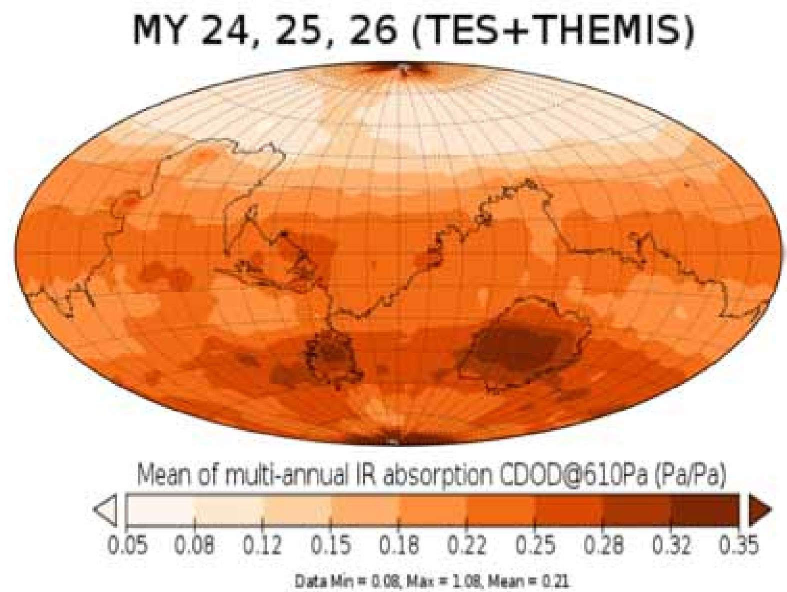

Montabone et al., 2017

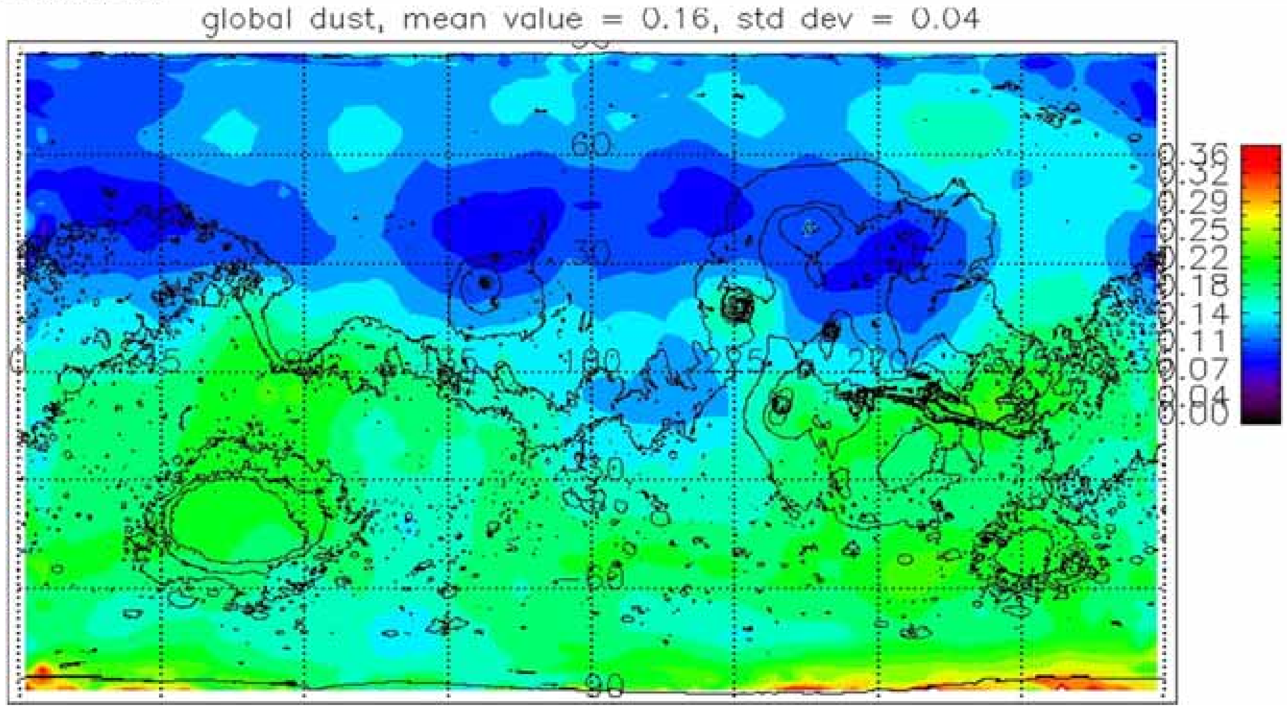

A global spatial map of dust distribution from MY 28 until MY 32 obtained from PFS measurements to be consistent with maps obtained by Montabone et al. 2017.

Dust activity in different Martian years observed by PFS

Global dust storm in MY28

Max. 2.14

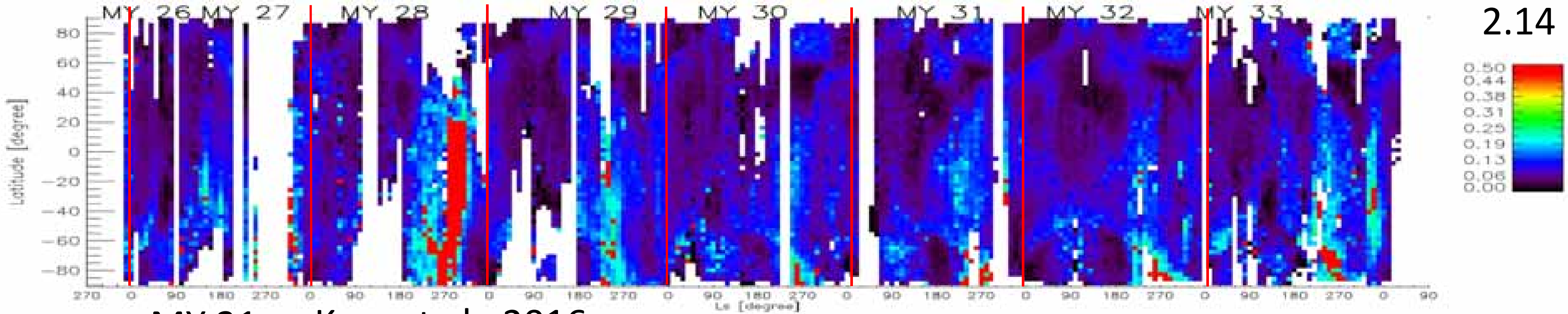

MY 31 Kass et al., 2016

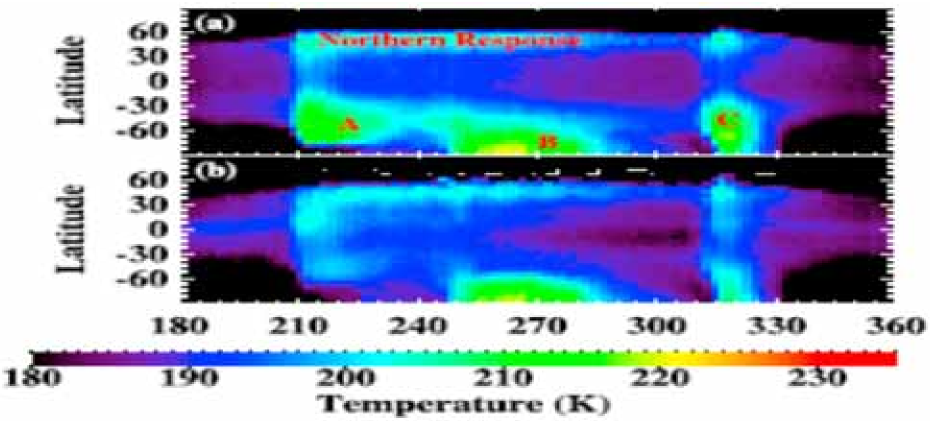

- Temperatures at 0.5 mb are consistent for both instruments
- All MYs except of MY 28 and MY 29 are included in figures below
- C storm is observed in PFS dust opacities during night at the same Ls, during day it occurs later
- B storm is clearly observed in PFS dust opacities
- A storm is weakly recognized in PFS dust opacities

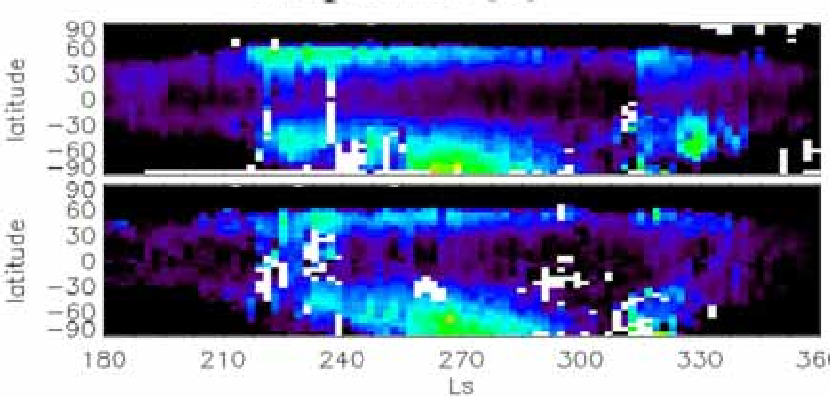

PFS Temperatures dayside (upper panel) and nighttime (bottom panel) at 0.5 mb

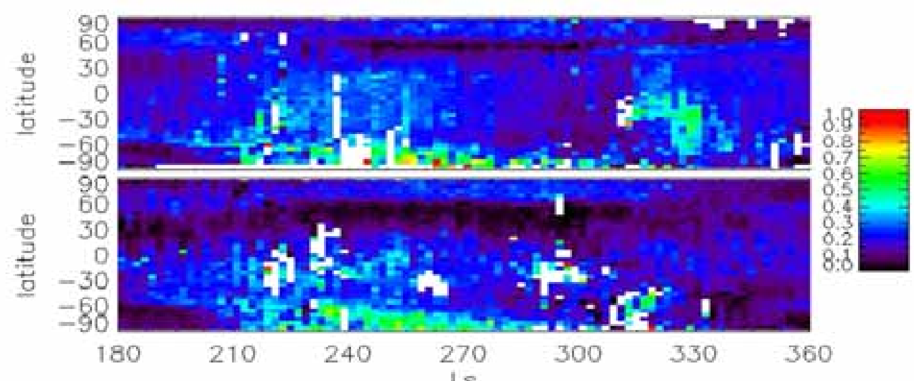

PFS dust opacities dayside (upper panel) and nighttime (bottom panel) normalized to 6.1 mb

Dust activity in dusty season (no global DS)

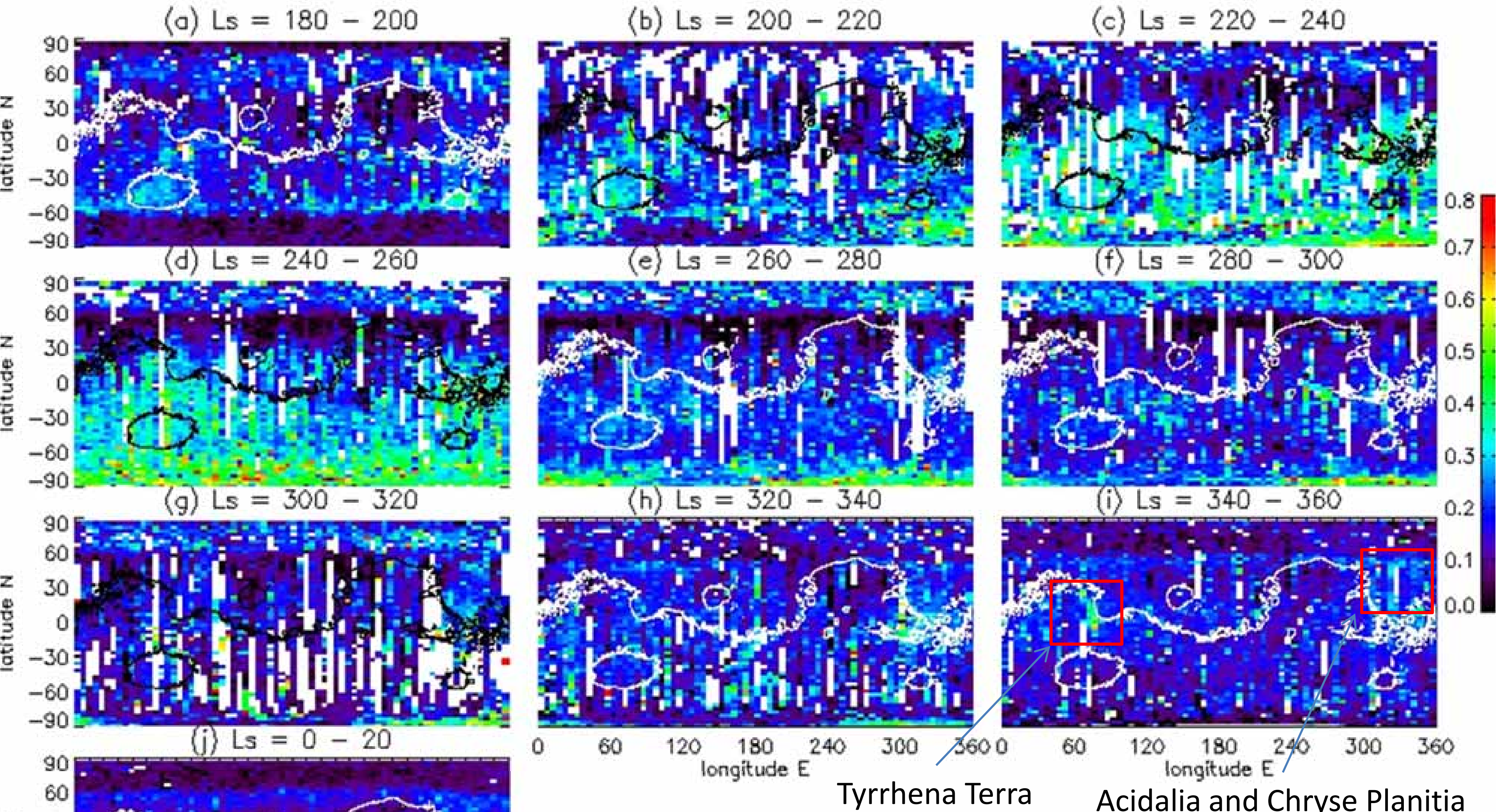

- Small regional dust storms develop over Hellas, Tyrrhena Terra, Argyre and high northern latitudes at Ls = 180° – 200°
- Maximum dust activity is observed at Ls = 240°-260°
- Quite clear atmosphere is evident over northern mid-latitudes (30°N - 60°N) from Ls = 220°-300°

Dust activity in MY 28 global DS

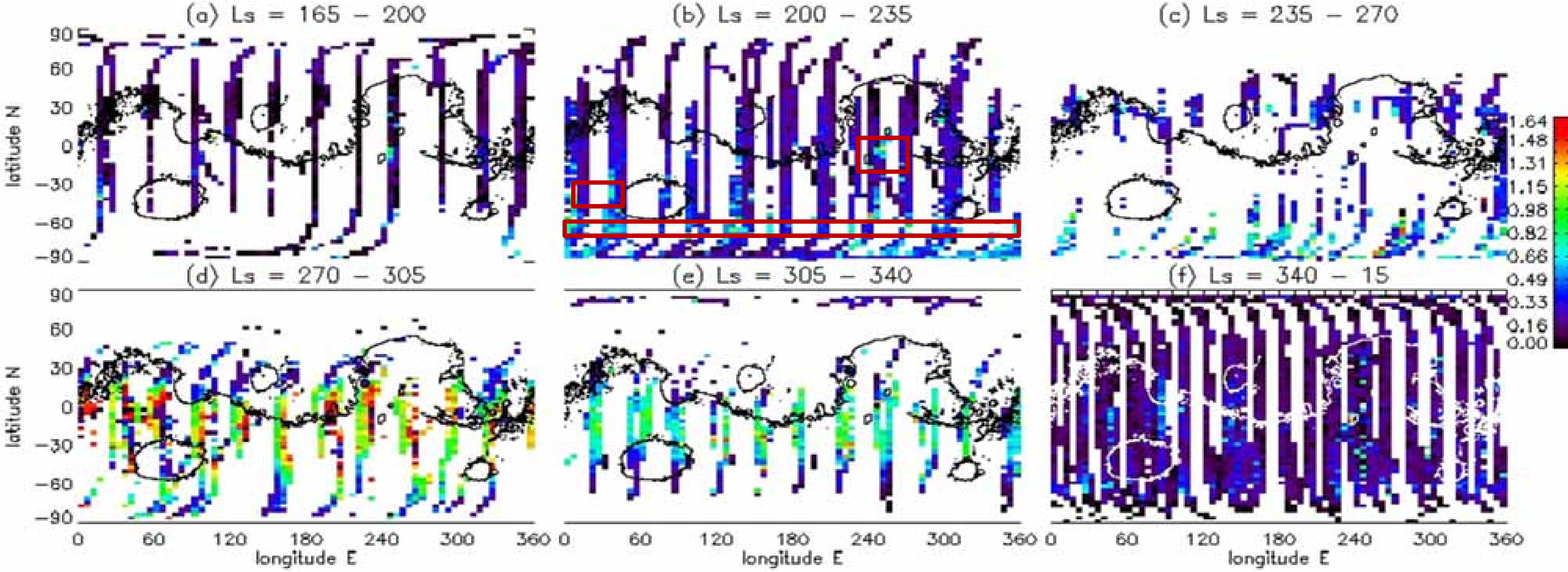

Possible precursor signal to the global dust storm

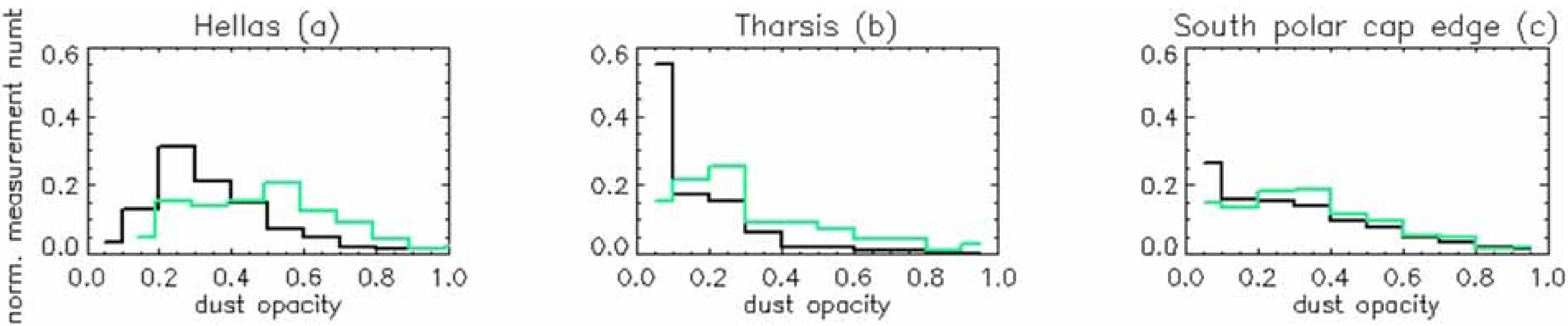

Histograms for specific regions for MY 28 (green) and other MYs (black)

In MY 28 some increases of dust opacity over specific locations (west of Hellas, Tharsis, South polar cap edge) are observed during Ls = 200° – 235° while the onset of global dust storm starts later (Ls = 260° – 267°) (Smith, 2009; Wang and Richardson, 2015) which is consistent with PFS observations.

Net heating and cooling rates due to atmospheric dust

Approach:
infrared range (~9 µm)
visible range (~ 0.67 µm),

$$\frac{dT}{dt} = \frac{Q}{\rho \cdot c_p} = \frac{g}{c_p} \cdot \frac{d\tau_\lambda}{dp} \cdot \frac{dF_\lambda(p)}{d\tau_\lambda}$$

Sanchez-Lavega, 2010

Orbit	Ls	LT	Location	Dust opacity at 1075 cm^{-1}
4510	273°	12.13	27°S, 117°E	1.73±0.06
4471	266°	12.18	42°S, 17°W	1.46±0.06
4328	241°	14.22	40°S, 3°W	0.41±0.06
4428	259°	12.82	34°S, 111°W	0.16±0.06

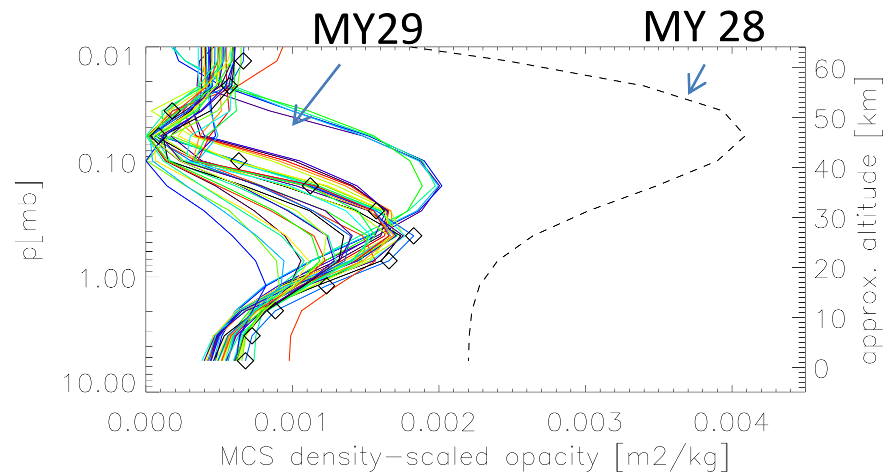

Heavens et al., 2011

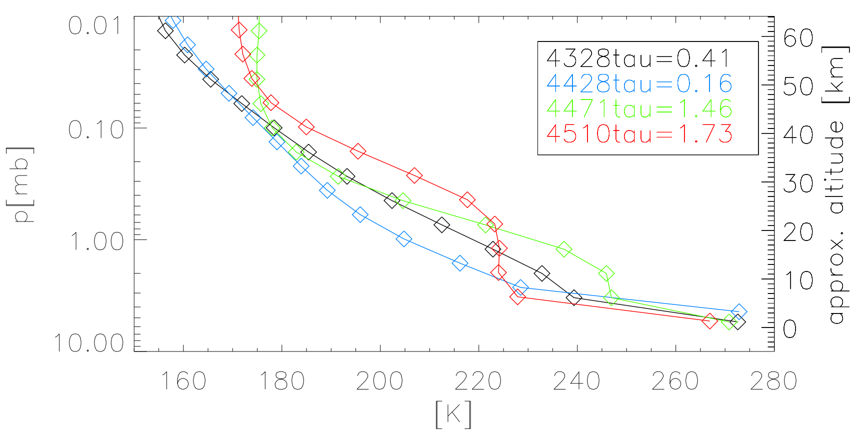

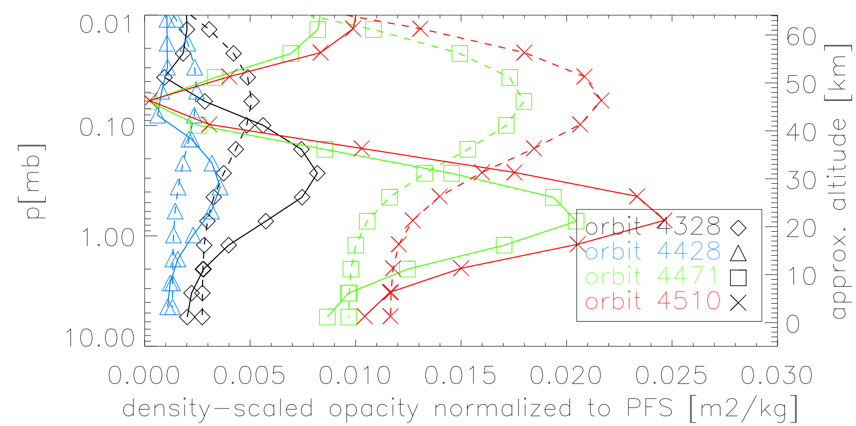

Net heating and cooling rates due to atmospheric dust

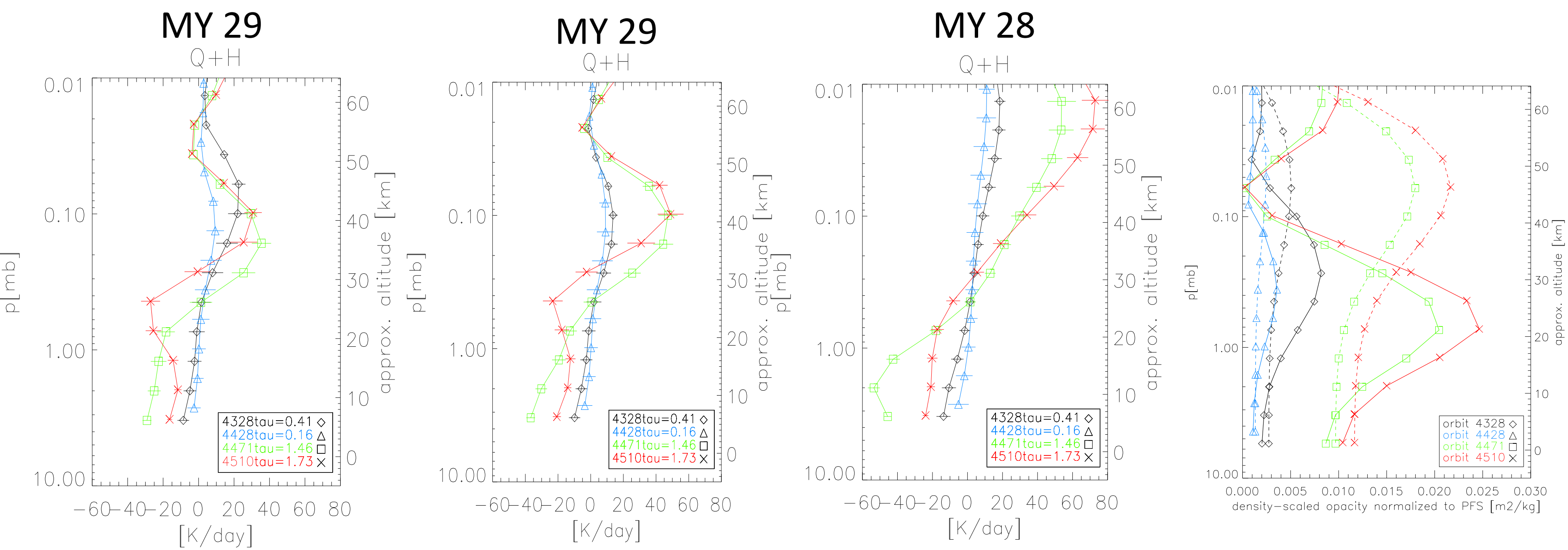

Closest approach | Typical approach | Dust vertical distribution from MY 28

- Heating rates increase with dust contents in the atmosphere and show maximum at ~ 40 km for MY 29 and ~ 60 km for MY 28, it is ~15 km above a peak of dust vertical distributions
- Maximum of cooling rates is observed for the modest-high dust opacity (1.46) close to the surface
- Anti-greenhouse effect (cooling at the surface, warming within the atmosphere) is observed and strongly increases with dust loads below ~30 km

Conclusions

- PFS dust opacities are consistent with data from other instruments (TES, THEMIS and MCS)
- The maximum activity of global dust storm occurred in MY 28 (Ls = 270° – 305°), later than for dust storms in other MYs (Ls = 240° – 260°)
- We found that regions of high topographic variations are mostly locations of onset for global in MY28 and also other dust storms in other MYs.
- Calculations of dust effect on the atmosphere have shown a strong heating at high altitudes (~ 40 – 50 km) above the dust vertical distribution peak
- High net cooling rates are observed for atmospheric layers close to the surface up to the dusty layer for the modest – high value of total opacity (1.46)